

# We are IntechOpen, the world's leading publisher of Open Access books Built by scientists, for scientists

6,900

Open access books available

185,000

International authors and editors

200M

Downloads

Our authors are among the

154

Countries delivered to

TOP 1%

most cited scientists

12.2%

Contributors from top 500 universities



WEB OF SCIENCE™

Selection of our books indexed in the Book Citation Index  
in Web of Science™ Core Collection (BKCI)

Interested in publishing with us?  
Contact [book.department@intechopen.com](mailto:book.department@intechopen.com)

Numbers displayed above are based on latest data collected.  
For more information visit [www.intechopen.com](http://www.intechopen.com)



# Quantification of Feeding Regions of Hypoeutectic Al-(5, 7, 9) Si-(0-4)Cu (wt.%) Alloys Using Cooling Curve Analysis

*Gerhard Huber, Mile B. Djurdjevic and Srećko Manasijević*

## Abstract

This chapter presents the potential of the cooling curve analysis to characterize the solidification path of the cast hypoeutectic series of Al-Si-Cu alloys and to quantify their feeding regions. The aim of this work is to examine how variations in the chemical composition of Si (5, 7 and 9 wt.%) and Cu (from 0 to 4 wt.%) might affect the characteristic solidification temperatures, their corresponding fraction solid, and feeding regions of investigated alloys. These parameters collected from the cooling curve analysis can be used for better understanding of the solidification paths of Al-Si-Cu alloys and could easily be incorporated into existing simulation software packages to improve their accuracy.

**Keywords:** aluminum alloys, thermal analysis, cooling curves, fraction solid, feeding

## 1. Introduction

Al-Si-Cu casting alloys show a great promise for several fields of engineering applications. Over the past few years, these alloys have been widely used in the automotive industry due to their suitable properties such as their lightness, strength, recyclability, corrosion, resistance, durability, ductility, formability and conductivity. Their good metallurgical properties, such as castability and fluidity, further enhance the applicability of these alloys for the production of intricate castings such as, e.g., the engine parts and cylinder heads. The chemical compositions of these alloys have a significant impact on all of the aforementioned properties. The alloying elements are usually added with the intent to improve the specific properties of casting parts. The main alloying elements: Si and Cu are primarily responsible for defining the microstructure and mechanical properties of aluminum alloys [1–7]. The castability and fluidity of these alloys have improved through Si addition. Additionally, the presence of Si leads to the reduction of shrinkage porosity, giving those alloys superior mechanical and physical properties.

Copper, as a second major alloying element, has been added to considerably increase strength and hardness of Al-Si-Cu alloys in as cast and heat-treated conditions. In addition, Cu reduces the corrosion resistance of aluminum alloys, and in certain alloys increases stress corrosion susceptibility. This element is generally

responsible for reducing the casting characteristics, especially the feeding ability of Al-Si-Cu alloys [8–10].

Any cast aluminum alloy during the transition from liquid to solid condition characterizes reduction in its volume. That reduction is usually in the range between 4 and 8 wt.% (higher Si content corresponds to lower reduction in the volume and vice versa). In order to eliminate the potential formation of shrinkage porosity by maintaining a path for fluid flow from the higher heat mass and the pressure of the riser to the isolated liquid pool, cast parts need to be additionally fed with a new volume of the liquid melt. According to Campbell [11], during directional solidification, it can be recognized five feeding mechanisms. They are, as **Figure 1** illustrates liquid feeding, mass feeding, interdendritic feeding, burst feeding, and solid feeding [11].

The liquidus ( $T_{liq}$ ), dendrite coherency temperature ( $T_{DCT}$ ), rigidity ( $T_{Rigidity}$ ) and solidus temperature ( $T_{sol}$ ) are important characteristic solidification temperatures of any aluminum alloys, which could be successfully used to delineate transition between various types of feeding mechanisms. All of these characteristic solidification temperatures, as **Figure 2** illustrates, can be easily determined using the thermal analysis (TA) technique [12]. The TA has been used for many years in aluminum casting plants as a quality control tool [3, 4, 13–28]. There are many reasons why this more than hundreds of years old technique has commercially

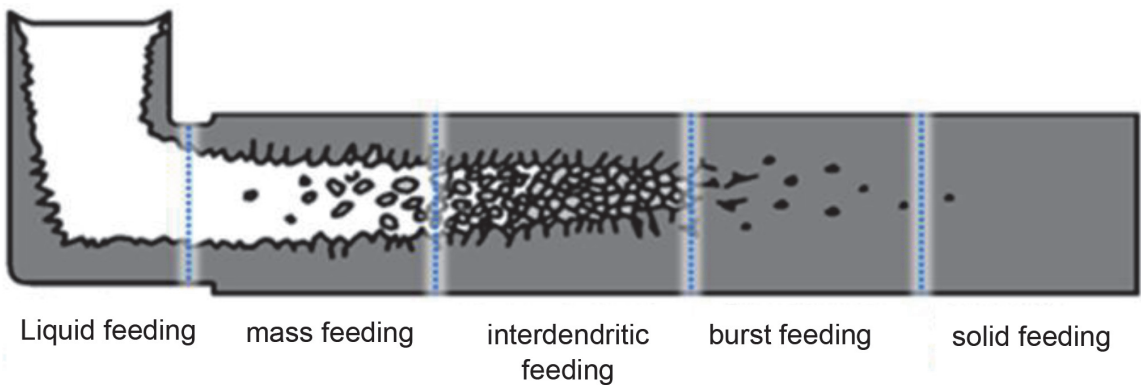


**Figure 1.**  
*Five feeding mechanisms recognized during directional solidification.*

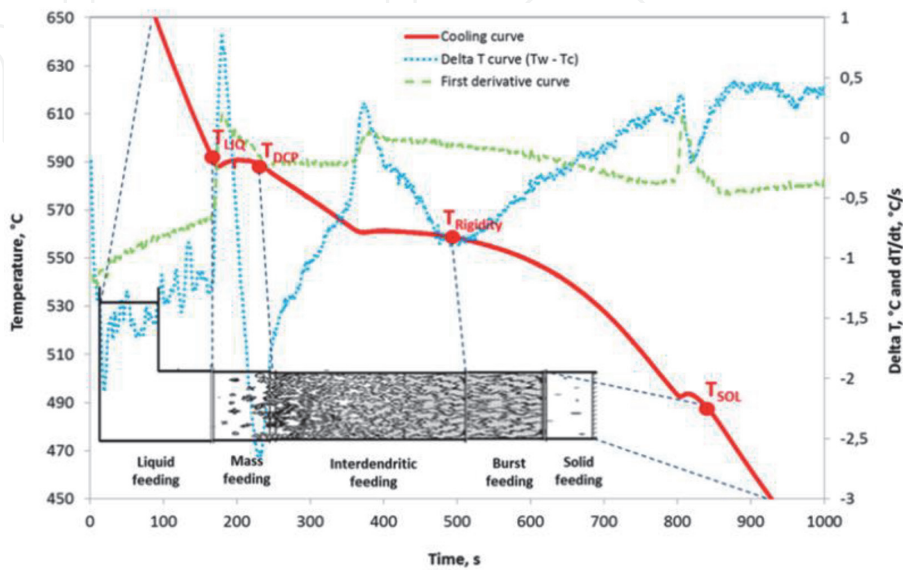


**Figure 2.**  
*Characteristic solidification temperatures, determined from the cooling curve, are bordering five feeding mechanisms.*

applied at numerous aluminum foundry plants. The TA method is simple, inexpensive and provides consistent results. Applying thermal analysis technique some fundamental relationship between cooling or its derivatives curves characteristics, alloy composition and melt treatment can be easier recognized and even better understood. Additionally, the first derivative of the cooling curve has been applied to calculate solid fraction distribution between  $T_{\text{liq}}$  and  $T_{\text{sol}}$  temperatures [29, 30].

Depending on the solidification interval of alloys, chemical compositions, cooling rates, amount of master alloys, hydrogen content and other, Al-Si-Cu alloys are prone to developing a considerable amount of shrinkage porosity. The solidification interval of Cu free alloys is very narrow; typically around 60°C, containing approximately 50% eutectic liquid. Usually, the level of porosity in such type of aluminum alloys is very low due to no feeding constraint during solidification of the last portion of eutectic liquid. The presence of Cu in the aluminum silicon alloys considerably extend their solidification range (reaching more than 100°C), making them more prone to the formation of shrinkage porosity [31].

Recently, it has shown [31, 32] sensitivity of aluminum-silicon alloys to porosity based on the content of Cu in these alloys. Addition up to 1 wt.% of Cu resulted in a significant increase in the porosity level. Surprisingly, further Cu addition up to 4 wt.% did not have such a significant impact on the porosity level at the same aluminum silicon alloy. It looks that development of porosity by cast aluminum-silicon alloys does not depend only on the concentration of Cu. It is also still not entirely clear which feeding regions is more responsible for the formation of shrinkage porosity. The impact of various major alloying elements (Si and Cu) on the feeding regions has not yet been fully analyzed. There is a lack of data, in the available literature, regarding quantification of feeding regions. The objective of this work is to examine how variation in chemical composition of Al-(5, 7, 9)Si-(0-4)Cu (wt.%) alloy may affect its characteristic solidification temperatures and corresponding fraction solid related to each temperature, as well as to quantify the effect of various contents of Si and Cu on the corresponding feeding regions. This analysis should help foundry professionals to understand better which feeding regions are more responsible for the formation of shrinkage porosity. To accomplish this, several experimental tests were carried out by applying the TA technique. All experimentally obtained data (the characteristic solidification temperatures and solid fraction) will be applied to quantify the five feeding regions of these alloys.

## 2. Experimental procedure

Twenty-five different Al-Si-Cu alloys with the chemical compositions, as presented in **Table 1**, are synthetically produced. Pure aluminum (commercial purity 99.7 wt.%) and pure copper (commercial purity 99.9 wt.%) have been used as impure materials. The content of the main alloying elements varied between 4.96–8.93 wt.% of Si and 0.0–4.30 wt.% of Cu. Their chemical compositions have been determined using optical emission spectroscopy (OES).

The alloys were melted in an electric resistance furnace, capacity 8 kg. No grain refining and modifier agents were added to the melt. During all experiments, degassing was not applied. Samples with masses of approximately 250 g were poured into coated stainless-steel cups. The height of the thermal analysis test cup was 60 mm, its diameter was 50 mm, while the weight of the steel test cup was 50 g.

Two calibrated commercial N type thermocouples with an accuracy of  $\pm 0.10^\circ\text{C}$  were inserted into thermal analysis cup and used during all experiments. One thermocouple was placed in the center of the thermos analysis cup while second

Alloy	Si	Cu
Al-5Si	4.96	0
Al-5Si-1Cu	5.22	1.12
Al-5Si-2Cu	5.12	1.88
Al-5Si-3Cu	5.08	3.11
Al-5Si-4Cu	5.01	4.30
Al-7Si	6.80	0
Al-7Si-1Cu	7.32	0.89
Al-7Si-2Cu	7.32	2.04
Al-7Si-3Cu	7.32	3.28
Al-7Si-4Cu	7.13	4.30
Al-9Si	8.80	0
Al-9Si-1Cu	8.93	0.92
Al-9Si-2Cu	8.93	2.17
Al-9Si-3Cu	8.82	2.93
Al-9Si-4Cu	8.92	4.02

**Table 1.**  
*Actual chemical composition (in wt.%) of synthetic Al-Si-Cu alloys.*

5 mm away from the cup inner wall. They recorded temperature during solidification of an investigated alloy (especially between 750 and 400°C temperature range). The National Instrument data acquisition system has been applied to collect temperature-time data. During all trials, the sampling rate was five data per second. The cooling conditions were maintained constant during all experiments, but due to various Si and Cu contents, the solidification rates slightly varied between maximal 0.26°C/s for Al-5Si-4Cu (wt.%) alloy and minimal 0.11°C/s for Al-9Si (wt.%) alloy. The cooling rate has been calculated as the ratio of the temperature difference between  $T_{liq}$  and  $T_{sol}$  to the total solidification time between these two temperatures. Each TA trial was repeated two times. Consequently, a total of 50 cooling curves were gathered.

3. Results and discussion

Porosity is one of the most common defects in aluminum cast parts caused mostly due to insufficient feeding and hydrogen precipitation during solidification. The amount of dissolved hydrogen in cast Al-Si alloys can be kept very low by degassing the melt. However, shrinkage porosity can still be a problem in the cast parts caused by non-proper feeding ability. Consequently, understanding the feeding behavior of hypoeutectic Al-Si-Cu alloys is an important aspect of sound casting production. In this paper, the impact of various contents of Si and Cu on different feeding regions has been analyzed by applying the TA technique. The main objective of this work was to better understand their impact on the feeding ability of Al-Si-Cu alloys and to quantify each feeding region regarding the characteristic solidification temperatures and/or the corresponding amount of fraction solid precipitated between those temperatures.

3.1 Analysis of characteristic solidification temperatures

The results of the cooling curve analysis are summarized in **Table 2**. The values of characteristic solidification temperatures ( $T_{liq}$ ,  $T_{DCT}$ ,  $T_{Rigidity}$  and  $T_{sol}$ ) have been determined from the cooling curves or their corresponding first derivatives curves. The dendrite coherency [3] and rigidity [12] temperatures have been determined by applying the two thermocouples method (one thermocouple located at the center

Alloy	$T_{liq}$	$T_{DCP}$	$T_{Rigidity}$	$T_{sol}$
Al-5Si	632.9	624.1	575.7	553.4
	634.2	624.9	576.7	555.5
Al-5Si-1Cu	631.5	623.1	571.4	500.1
	628.1	623.4	571.7	499.7
Al-5Si-2Cu	625.4	619.5	567.2	497.8
	624.9	619.1	568.0	496.8
Al-5Si-3Cu	622.5	616.2	562.8	500.6
	621.8	617.0	562.0	499.2
Al-5Si-4Cu	617.0	613.2	558.7	498.5
	617.1	613.2	558.7	501.9
Al-7Si	617.8	610.7	576.7	552.0
	617.6	611.5	576.8	553.4
Al-7Si-1C	612.6	604.5	573.8	498.0
	611.8	604.5	574.0	497.9
Al-7Si-2Cu	607.4	602.3	570.6	495.3
	607.2	603.3	570.2	495.0
Al-7Si-3Cu	603.5	598.0	567.1	494.3
	603.2	596.8	566.5	494.0
Al-7Si-4Cu	599.6	594.0	563.4	497.1
	599.1	593.6	563.8	496.1
Al-9Si	600.2	595.7	575.0	549.3
	600.5	597.6	575.2	552.3
Al-9Si-1Cu	597.3	593.9	573.1	494.7
	595.8	593.7	572.,4	493.6
Al-9Si-2Cu	591.9	589.,2	569.5	493.6
	591.9	589.6	569.6	494.5
Al-9Si-3Cu	589.4	587.2	567.1	492.7
	588.7	587.0	566.5	493.7
Al-9Si-4Cu	582.8	581.8	564.8	493.0
	582.4	581.7	564.6	492.6

Two sets of the characteristic temperatures have been collected for each analyzed alloy (two cooling curves have been collected for each alloy).

**Table 2.**  
Characteristic solidification temperatures of Al-(5, 7, 9)Si-(0-4)Cu (wt.%) alloys determined using cooling curve analysis.

( $T_c$ ) and second ( $T_w$ ) placed nearby the inner wall of test cup). Characteristic solidification parameter such as dendrite coherency point (DCP) has determined by identifying the first local minimum on the delta  $T$  curve ( $\Delta T = T_w - T_c$ ) plotted versus time. The dendrite coherency temperature (DCT) has detected by reading the temperature on the cooling curve for the corresponding time related to dendrite coherency point [3]. It has recently been found that the second local minimum on the  $\Delta T$  versus time curve is related to the  $T_{Rigidity}$  [12]. The reason that DCP and rigidity occur at these minimums of the  $\Delta T$  curve is because the heat removal from the solid is faster than from the liquid phase. This is due to the significantly higher thermal conductivity of the solid dendrites by DCP and solid dendrites and eutectic cells by rigidity in comparison to the surrounding liquid metal.

The  $T_{liq}$  specifies the maximal temperature at which the crystal can coexist with the melt in thermodynamic equilibrium. Above the  $T_{liq}$  there is not a single crystal and the melt is liquid and homogeneous. From **Table 2** and **Figure 3**, it is evident

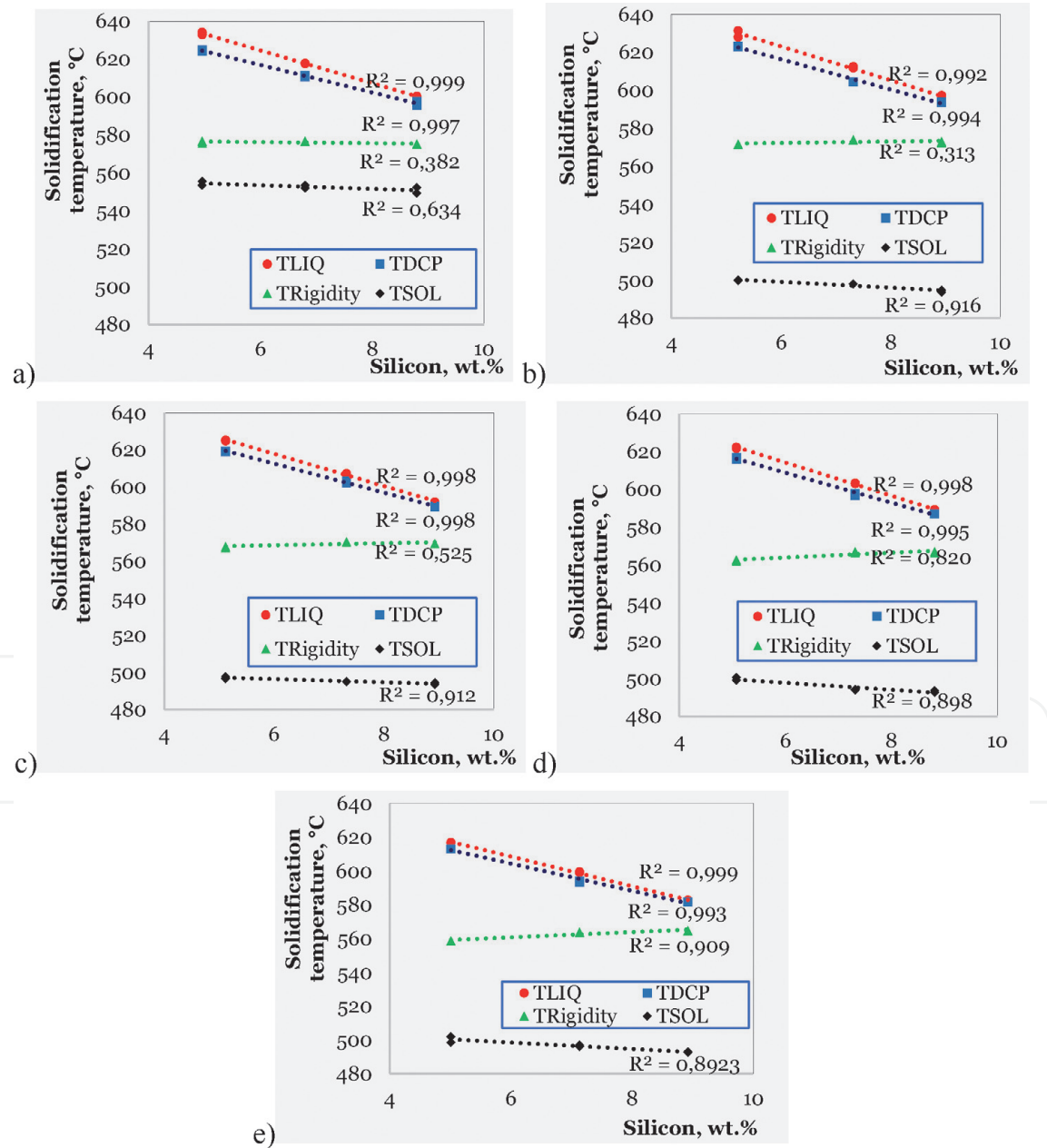


**Figure 3.** The impact of Si on the characteristic solidification temperature: (a) Al-(5, 7, 9)Si-0Cu (wt%), (b) Al-(5, 7, 9)Si-1Cu, (c) Al-(5, 7, 9)Si-2Cu (wt%), (d) Al-(5, 7, 9)Si-3Cu (wt%) and (e) Al-(5, 7, 9)Si-4Cu (wt%) alloys.

that any increase in the content of Si and Cu significantly depressed the liquidus, dendrite coherency, and rigidity temperatures, while solidus temperature is less prone to their influence. According to the results obtained using the cooling curve analysis, the increase in Si content by one weight percent depresses the  $T_{liq}$  to 8.5°C by the constant content of Cu. The experimental result indicated the stronger impact of Si on the  $T_{liq}$  in comparison with that obtained using the binary Al-Si phase diagram. Calculated from the binary phase diagram, increase of Si content up to eutectic concentration (~12.0 wt.%) decreases the  $T_{liq}$  by 83°C (the temperature drops almost linearly from 660 to 577°C), which is approximately a decrease of 7°C per 1 wt.% of Si. One weight percent of Cu by constant content of Si decreases the  $T_{liq}$  by approximately 4.4°C, which is a higher value than expected according to the equilibrium binary Al-Cu phase diagram (3.4°C/1 wt.% of Cu). The most plausible reason for these differences can be found in the fact that in all experiments, a limited range of Si (up to 8.9 wt.%) and Cu (up to 4.3 wt.%) content has been analyzed in comparison with significantly broader concentration ranges (up to 12 wt.% for Si and up to 33 wt.% for Cu) taken from the binary Al-Si and Al-Cu phase diagrams. At the same time, the impact of higher cooling rates during some experiments (~0.26°C/s) cannot be disregarded, which certainly depressed the  $T_{liq}$  to a lower value.

During the solidification of any aluminum hypoeutectic Al-Si-Cu alloys, a dendritic network of primary  $\alpha$ -aluminum crystals will be developed. However, as the melt cools, the dendrite tips of the growing crystals begin to impinge upon one another until a coherent dendritic network is formed [4]. The temperature at which the dendrite tips start to touch each other is called dendrite coherency temperature  $T_{DCT}$ . This temperature is a very important feature of the solidification process because it marks the moment when the “mass” feeding is transferred to the interdendritic feeding [33–42]. According to many researchers, casting defects such as macrosegregation, shrinkage porosity and hot tearing begin to develop after the  $T_{DCP}$  [33–37]. The solidification conditions, the chemical compositions of alloy and the addition of grain refiners are major factors that have a significant impact on the DCT. Regardless of the applied measurement techniques, it has been verified that faster cooling rate and increase in solute concentration postponed the coherency point for the lower temperature [36, 37, 41]. From **Table 2** and **Figure 3**, it is obvious that the higher Si and Cu contents progressively reduce the DCT. The impact of Si is more significant than that of Cu. For the Cu free alloys, 1 wt.% of Si decreases the DTC to ~7.2°C, while by alloys with various content of Cu (from 1 to 4 wt.%) that decrease is slightly higher and is approximately 7.9°C. Each increase in the Cu content by 1 wt.% in analyzed alloys will decrease the DCT to approximately 3.2°C. These results are not unexpected and are consistent with the available literature data [37, 39]. According to literature data, the size of secondary dendrite arms mostly depends on the local cooling rates and the amount of alloying elements present in the melt. The impact of the local cooling rate is very well studied; a higher cooling rate relates to the smaller dendrites and vice versa. The effect of alloying elements on the size of dendrite arm spacing needs to be also considered due to their not even distribution in the liquid and solid phases. Excess amount of solute displaced away from the solidification interface into the melt results in an increase in the volume of solute located between already formed dendrite arms. The resulted constitutional undercooling (supersaturation) is an additional driving force for the growth of the dendrites. In order to accommodate an excess amount of solute elements, the space between primary  $\alpha$ -aluminum dendrites must be increased. The higher concentration of alloying elements will reduce the growth of secondary dendrites and postpone their contact-coherency to lower temperature. Based on the

previously mentioned, it could be assumed that elements with a lower solubility in the aluminum melt are more effective in reducing the size of secondary dendrite arm spacing (SDAS). Therefore, the effect of the same content of Cu (max. solubility in Al is 5.7 wt.%) is significantly lower than the effect of the same amount of Si (max. solubility in Al is 1.6 wt.%).

The rigidity point/temperature indicates the moment during solidification at which the flow of residual melt through interdendritic channels is completely restricted. As **Figure 2** shows, the  $T_{\text{Rigidity}}$  has been determined as the second minimum on the  $\Delta T$  curve ( $\Delta T = T_w - T_c$ ) that are identified in the region of primary precipitation of Al-Si eutectic. Again, the most likely main reason for this difference is due to different thermal conductivity in solid and liquid phases. The rigidity point indicates the moment when the interdendritic feeding is transferred to burst feeding. According to Campbell [11], after the rigidity point, the stress will exceed the network strength and the dendritic network will collapse.

From **Table 2** and **Figure 3**, it is obvious that any changes in the content of Si have no significant impact on the value of  $T_{\text{Rigidity}}$ . Small changes in this temperature ( $\pm 0.5^\circ\text{C}$ ) could be related to the accuracy of applied thermocouples. On the contrary to that, the addition of Cu (up to 4 wt.%) to Al-Si alloys depressed this temperature to approximately  $3.2^\circ\text{C}$  per one weight percentage of Cu. It is interesting to note that by a lower content of Si (5 wt.%) the depression is stronger ( $\sim 4.0^\circ\text{C}/1\text{ wt.\% Cu}$ ) than by alloys with higher Si (9 wt.%) content ( $2.5^\circ\text{C}/1\text{ wt.\% of Cu}$ ).

Finally, the  $T_{\text{sol}}$  identifies the temperature at which the last portion of the liquid has been transformed into a solid. Below this temperature, the given alloy is stable in the solid phase. The results presented in **Table 2** and **Figure 3** indicate that various Si and Cu contents in investigated alloys have the lowest impact on solidus temperature. The average  $T_{\text{sol}}$  determined using cooling curve analysis, for all investigated alloys, was approximately  $500^\circ\text{C}$ .

The addition of Si and Cu into aluminum alloys considerably changes the solidification ranges of these alloys (the difference between  $T_{\text{liq}}$  and  $T_{\text{sol}}$ ). The Al-Si alloys free of Cu, as **Figure 3** illustrates, solidified in the temperature range between  $80$  and  $50^\circ\text{C}$  depending on the content of Si. The lower Si content corresponds to the wider solidification interval of these alloys and vice versa. Addition of Cu into Al-Si alloys, as **Figure 3** shows, significantly increases their solidification intervals. By lowering the contents of Si (e.g., 5 wt.%) and Cu (e.g., 1 wt.%) this interval is approximately  $130^\circ\text{C}$ , getting narrower ( $\sim 90^\circ\text{C}$ ) by increasing the contents of Si (e.g., up to 9 wt.%) and Cu (e.g., up to 4 wt.%). It is well known that casting characteristics of Al-Si-Cu alloys are generally influenced upon adding Cu. The Cu precipitate in the eutectic form during the last stage of solidification prolonging solidification interval of those alloys [31]. It is also well known from the foundry practice that alloys with wider solidification intervals are more prone to the formation of shrinkage porosity.

### 3.2 Fraction solid analysis

The term fraction solid is related to the amount of solid phase(s) formed during melt solidification between liquidus and solidus temperatures, expressed in percentage. Correct information regarding fraction solid is necessary to accomplish computer simulation of casting feed ability as well as to characterize the solidification process and make a prediction concerning the casting structure.

Various methods for determining the fraction solid of casting alloys are presented in the literature [30–38]. The most commonly used technique employs quantitative metallography. The image analysis system is used to measure the

volume fraction of phases formed prior to quenching in a set of melt specimens obtained between the  $T_{liq}$  and  $T_{sol}$ . This technique requires the use of small samples that have rapid cooling rates in order to preserve the structure present at a given temperature. Small test samples and rapid cooling rates minimize structural transformation during quenching and thus maximize the accuracy of this measurement procedure. Another approach for determining fraction solid makes use of the TA technique [3, 4, 17, 25, 26, 28–30, 43–52]. The amount of heat evolved from a solidifying test sample can be calculated as the integrated area between the first derivative curve and the zero line. The amount of heat is proportional to the fraction solid. Differential thermal analysis (DTA) and differential scanning calorimetry (DSC) have also been used for the determination of solid fraction. However, these techniques are not suitable for industrial applications because they require complicated and expensive instrumentation as well as rigid and precise test procedures that are only possible in a laboratory environment. The literature also suggests a number of models for the calculation of fraction solid (more details can be found in **Table 3**). Most of them are based on parameters derived from the fundamental analysis of the solidification process for simple alloy systems. Due to the highly complex nature of alloy solidification, many questionable assumptions (see **Table 3**, comments) have been made in these models.

The TA technique has been applied in this work to calculate the distribution of fraction solid between the  $T_{liq}$  and  $T_{sol}$  during solidification of investigated alloys.

No	Type of models	Method	Comments
1.	$f_s = \frac{T_{liq}-T}{T_{liq}-T_{sol}}$ $T_{liq}$ —liquidus temperature, °C $T_{sol}$ —solidus temperature, °C $T$ —instantaneous temperature, °C	LINEAR [30]	Latent heat is assumed to vary linearly between liquidus and solidus temperatures. This model has no theoretical basis but is frequently used due to its simplicity.
2.	$f_s = \frac{1}{1-k} \frac{T_{liq}-T}{T_m-T}$ $k = \frac{T_m-T_{liq}}{T_m-T_{sol}}$ $k$ —distribution coefficient of binary alloys $T_m$ —melting temperature of pure aluminum	LEVER RULE [30]	Solidification in this model is assumed to progress very slowly and the solid and liquid phases coexist in equilibrium in the mushy zone.
3.	$T_{E,G}^{AlSi} < T < T_{liq}$ $f_s = 1 - \left( \frac{T_m-T}{T_m-T_{liq}} \right)^{\frac{1}{k-1}}$ $T_{E,G}^{AlSi}; f_s = 1$	SCHEIL'S [30]	In this model, it is assumed that no solute diffusion occurs in the solid phase and also that the liquid is perfectly homogeneous.
4.	$f_s = 1 - \exp\left(-\frac{4}{3}\pi R^3 N\right)$ $R$ —average grain radius, m $N$ —average grain density, $m^{-3}$	GRAIN NUCLEATION [32, 37]	The calculation of fraction solid is based on the grain nucleation law and on the assumption that the shape of the grains is spherical.
5.	$f_s = \frac{\int_0^t \left[ \left( \frac{dT}{dt} \right)_{cc} - \left( \frac{dT}{dt} \right)_{zc} \right] dt}{\int_0^t \left[ \left( \frac{dT}{dt} \right)_{cc} - \left( \frac{dT}{dt} \right)_{zc} \right] dt} = \frac{c_p}{L} \int_0^t \left[ \left( \frac{dT}{dt} \right)_{cc} - \left( \frac{dT}{dt} \right)_{zc} \right] dt$ $c_p$ —specific heat of an alloy $L$ —latent heat of solidification $\frac{dT}{dt}$ —cooling rate	HEAT BALANCE [9, 10, 35, 37]	Fraction solid can be calculated by determining the cumulative area between the first derivative of the cooling curve (cc), and the “zero” cooling curve (hypothetical cooling curve without phase transformations) (zc).

**Table 3.**  
Review of models for calculation of fraction solid.

There are two known methods in the literature, Newtonian [29, 30, 52] and Fourier, [29, 30, 52] that have been successfully used to calculate fraction solid distribution using cooling curve analysis. In order to be capable of applying both methods, it is necessary to define the so-called baseline [29, 30, 52]. The baseline denotes the first derivative curve of the investigated alloy, assuming that melt during solidification process does not undergo any phase transformation. Therefore, it is to expect that base and first derivative curves are overlapping each other in the areas before liquidus (single liquid phase) and after solidus (single solid phase) temperatures. In this paper only the Newtonian method has been applied for calculating the base line using cooling curve analysis.

**Table 4** and **Figure 4** summarize the impact of various content of Si and Cu on the distribution of fraction solid at characteristic solidification temperatures ( $T_{\text{liq}}$ ,  $T_{\text{DCT}}$ ,  $T_{\text{Rigidity}}$  and  $T_{\text{sol}}$ ). For Cu free Al-Si alloys, as **Table 4** and **Figure 4** shows, an increase in the content of Si from 5 up to 9 wt.% lowering the amount of fraction solid at DCT for 50%, while the amount of fraction solid at  $T_{\text{Rigidity}}$  is only for 5% lower by higher silicon content. Addition of Cu into Al-Si alloys drastically changes the distribution of the fraction solid at characteristic solidification temperatures. By increasing the content of Cu from 1 up to 4 wt.%, the fraction solid at  $T_{\text{Rigidity}}$  decreased independently from the Si content to approximately 30% (from almost 90 to approximately 60%). At the same time, the addition of Cu does not have such a significant impact on the amount of fraction solid precipitated at the DCP. At lower content of Si, this impact is much stronger (fraction solid by adding Cu decreased to almost 10%), while by a higher content of Si, the impact is negligible (about 1%). According to **Table 4** and **Figure 4**, it appears that the alloy with a shorter solidification range (e.g., Al-9Si-4Cu (wt.%)) achieves both Dendrite Coherency and Rigidity points at a lower fraction solid (12% and 56%, respectively) compared to the alloy with wider freezing range (e.g., Al-5Si-1Cu (wt.%)) and consequently higher fraction solid values for these two points ( $\sim 24\%$  and  $\sim 84\%$ , respectively).

From **Figure 4**, it is obvious that with the Cu free Al-Si alloys, the interdendritic feeding region is dominantly independent of the content of Si in the investigated alloy. Increase in the Si content from 5 to 9 wt.% decreased the amount of fraction solid at the DCT from approximately 27% up to 13%. For the same increase of the Si content, the amount of fraction solid which precipitated at Rigidity point decreased from 94% to 89.5%. This means that around 70% of fraction solid precipitated during solidification between Dendrite Coherency and Rigidity temperatures. At the same time, an increase in the content of silicon from 5 to 9 wt.% decreases the amount of fraction solid by almost 50%, which precipitated between  $T_{\text{liq}}$  and  $T_{\text{DCT}}$ . The burst feeding region is getting slightly wider by adding Si into aluminum alloys. Addition of Cu into these Al-Si hypoeutectic alloys considerably changes the distribution of the fraction solid among feeding regions. The Cu significantly increases the presence of the burst feeding. With Al-5Si-5Cu (wt.%) alloy, the amount of fraction solid formed between Rigidity and Solidus temperatures was about 15%, while at Al-9Si-4Cu (wt.%) that amount was above 40%.

Simultaneously, the amount of fraction solid formed between  $T_{\text{DCP}}$  and  $T_{\text{Rigidity}}$  was noticeably reduced from 60% by Al-5Si-1Cu (wt.%) alloy up to 44% by Al-9Si-4Cu (wt.%) alloy. Generally, it can be noticed that the higher content of Cu significantly increases the existence of the burst feeding region, decreases the domain of interdendritic region and slightly reduces the mass feeding region. It is evident from **Figure 3** that the various Si content significantly depressed the DCT, while its impact on  $T_{\text{Rigidity}}$  could be neglected. Higher Si content decreased the solidification interval ( $T_{\text{liq}} - T_{\text{sol}}$ ) of those alloys, changing also their solidification mode. It is

Alloy	$F_s$ at			
	$T_{liq}$	$T_{DCP}$	$T_{Rigidity}$	$T_{sol}$
Al-5Si	0	27.5	95.2	100
		24.6	93.1	
Al-5Si-1Cu		26.0	85.7	
		23.2	82.5	
Al-5Si-2Cu		24.0	79.7	
		21.3	76.7	
Al-5Si-3Cu		19.3	73.7	
		17.6	74.7	
Al-5Si-4Cu		15.4	65.3	
		16.5	68.7	
Al-7Si		17.8	91.9	
		17.5	91.2	
Al-7Si-1Cu		16.7	76.4	
		18.7	78.2	
Al-7Si-2Cu		14.7	65.6	
		14.5	66.7	
Al-7Si-3Cu		14.5	61.8	
		15.8	65.5	
Al-7Si-4Cu		13.9	56.4	
		14.1	55.4	
Al-9Si		14.1	89.1	
		12.3	90.2	
Al-9Si-1Cu		12.2	73.1	
		13.1	77.8	
Al-9Si-2Cu		12.3	65.8	
		12.8	63.1	
Al-9Si-3Cu		13.3	61.3	
		13.8	60.1	
Al-9Si-4Cu		12.6	56.0	
		12.3	57.1	
Fraction solid values for the characteristic solidification temperatures have been collected for each analyzed alloy.				

**Table 4.**  
Characteristic fraction solid values of Al-(5, 7, 9)Si-(0-4)Cu (wt.%) alloys determined using cooling curve analysis.

evident that the alloying element may change feeding ranges ability by shifting the alloy characteristic solidification temperatures. This may cause either a widening or narrowing of the corresponding feeding ranges of the alloy. The Cu has an impact on both dendrite coherency and  $T_{Rigidity}$ , as shown in **Table 2**, by depressing them to lower values. It is also well known that copper increases the solidification interval of Al-Si alloys. It can be seen from **Figure 4** that increase in the content of Si

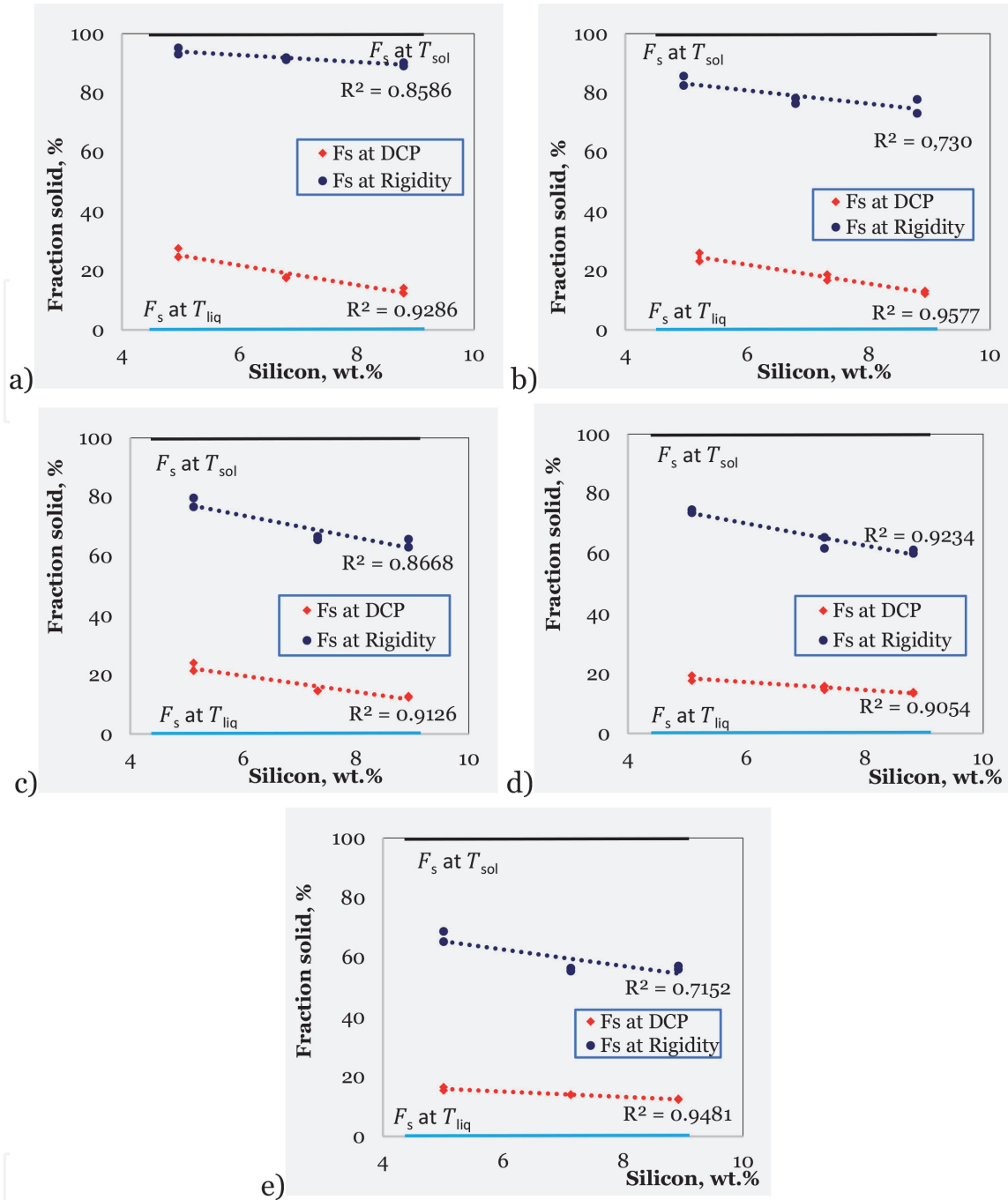


**Figure 4.**

The impact of Si on the fraction solid: (a) Al-(5, 7, 9)Si-0Cu (wt%), (b) Al-(5, 7, 9)Si-1Cu (wt%), (c) Al-(5, 7, 9)Si-2Cu (wt%), (d) Al-(5, 7, 9)Si-3Cu (wt%) and (e) Al-(5, 7, 9)Si-4Cu (wt%) alloys at the characteristic solidification temperatures.

(from 5 to 9 wt.%) and Cu (from 0 to 4 wt.%) significantly dropped down the amount of fraction solid at  $T_{Rigidity}$ , while the amount of fraction solid at DCT is slightly reduced. Besides chemical compositions, it is well known that other parameters have also been identified to affect the feeding capability of aluminum alloys [35–43]. Among these are melt superheat, temperature gradients during solidification, the influence of chemical composition, eutectic modification, grain refinement and hydrogen solubility. All these factors need to be taken into consideration in order to be able to properly answer which feeding region is more significant for the formation of cast defects. The correct answer could only be achieved if additional experimental techniques were introduced, such as the Tatur test sample, the measurement of the collecting temperature and the Hubler test sample, in addition to the thermal analysis. This paper has shown that applying cooling curve analysis to

all five feeding regions proposed by Campbell can be accurately quantified by either the temperature or corresponding fraction solid precipitated at those temperatures.

#### 4. Conclusion

In the available literature, information related to a quantitative description of the five feeding mechanisms proposed by Campbell is limited. In this paper, the impact of the main alloying elements Si and Cu on different feeding regions of hypoeutectic Al-Si-Cu cast alloys has been studied using the TA technique. It has been shown that both elements have a significant impact on the characteristic solidification temperatures as well as on the amount of fraction solid precipitated at given temperatures. This work has also shown that TA is a valuable tool widely used in aluminum foundries that can collect numerous parameters (characteristic solidification temperatures, fraction solid distribution and others), which are beneficial for a better understanding of the solidification path of hypoeutectic Al-Si-Cu alloys. Applying TA technique as presented in this paper, it is now possible to describe each feeding region quantitatively through a temperature difference related to the total solidification interval or through a different amount of fraction solid that precipitated in each region. It can be assumed that calculated fraction solid at the DCT and fraction solid at  $T_{\text{Rigidity}}$  together with corresponding characteristic solidification temperatures are useful parameters for performing computer simulations of casting feed ability and for the characterization of the solidification process of cast Al-Si-Cu alloys.

#### Acknowledgements

Publication of the manuscript is funded by the Lola Institute Ltd. ([www.li.rs](http://www.li.rs)).

#### Conflict of interest

All authors declare that they have no conflict of interest in this research.

#### Author details


Gerhard Huber<sup>1</sup>, Mile B. Djurdjevic<sup>1</sup> and Srećko Manasijević<sup>2\*</sup>

<sup>1</sup> Nemak Linz GmbH, Linz, Austria

<sup>2</sup> Lola Institute Ltd, Belgrade, Serbia

\*Address all correspondence to: [srecko.manasijevic@li.rs](mailto:srecko.manasijevic@li.rs)

#### IntechOpen

© 2019 The Author(s). Licensee IntechOpen. This chapter is distributed under the terms of the Creative Commons Attribution License (<http://creativecommons.org/licenses/by/3.0>), which permits unrestricted use, distribution, and reproduction in any medium, provided the original work is properly cited. 

## References

- [1] Mondolfo LF. Aluminum Alloys, Structure and Properties. London: Butterworths; 1979. pp. 213-614
- [2] Crossley PB, Mondolf LF. Modern Casting. 1966;**49**:53-64
- [3] Bäckerud L, Chai G, Tamminen J. AFS/Skanaluminium. 1986;**2**:95
- [4] Arnberg L, Backerud L. Solidification Characteristics of Aluminum Alloys, Vol. 3: AFS. Illinois USA: Des Plaines; 1996
- [5] Djurdjevic BM, Manasijevic S. Impact of alloying elements on the solidification parameters of cast hypoeutectic AlSi6Cu (1–4) and AlSi8Cu (1–4) alloys. Journal of Metallurgical and Materials Engineering. 2014;**20**(4):235-246
- [6] Huber G, Djurdjevic BM. Impact of silicon, magnesium and strontium on feeding ability of AlSiMg cast alloys. In: THERMEC; ; 29.05–03.06. 2016, Graz, Austria. 2016. p. 249
- [7] Djurdjevic BM, Manasijevic S, Odanovic Z, Radisa R. Influence of different contents of silicon and copper on the solidification pathways of cast hypoeutectic AlSi(5–9 wt.%) Cu(1–4 wt.%) alloys. International Journal of Materials Research. 2013;**104**(9):865-873
- [8] Djurdjevic BM, Huber G. Determination of rigidity point/temperature using thermal analysis method and mechanical technique. Journal of Alloys and Compounds. 2014;**590**:500-506
- [9] Djurdjevic BM, Odanovic Z, Zak H. Detection of dendrite coherency temperature by aluminum alloys using single thermocouple technique. Praktische Metallographie. 2012;**49**(2):86-98
- [10] Vicario I, Villanueva E, Djurdjevic BM, Huber G. Determination of dendrite coherency point characteristics using two new methods. Journal of Applied Sciences. 2018;**8**:1-14
- [11] Campbell J. AFS Cast Metal Research Journal. 1969;**5**(1):1-8
- [12] Djurdjevic MB, Huber G. Journal of Alloys and Compounds. 2014;**590**: 500-508
- [13] Huber G, Djurdjevic MB. Erweiterte Thermoanalyse mit Dendrite Coherency und Rigidity Punkt und deren mögliche neue Anwendungsgebiete. Giesserei Rundschau. Heft. 2014;**7**(8):223-234
- [14] Djurdjevic BM, Manasijević S, Dirnberger F. Macroscopic characterization of aluminum cast alloys using cooling curve analysis. Livarstvo-Foundry. 2013;**52**(2):2-11
- [15] Djurdjevic BM, Vicario I, Huber G. Review of the thermal analysis application in aluminum casting plants. Revista de Metalurgia. 2014;**50**:1-12
- [16] Huber G, Djurdjevic BM. Benefit of cooling curve analysis for simulation of aluminum casting process. In: Proceedings of MSE Congress: 25–27 September 2012, Darmstadt, Germany. 2012. pp. 1-12
- [17] Djurdjevic BM, Odanovic Z, Talijan N. Characterization of the solidification path of AlSi5Cu(1–4 wt.%) alloys using cooling curves analysis. Journal of Metals. 2011;**63**(11):51-57
- [18] Huber G, Djurdjevic BM, Odanovic Z. Synergy between thermal analysis and simulation. Journal of Thermal Analysis and Calorimetry. 2013;**111**:1365-1373
- [19] Djurdjevic BM, Manasijević S. Primena termičke analize u livnicama aluminijuma. Livarstvo-Foundry. 2013;**52**(1):28-36

- [20] Cibula A. Journal of the Institute of Metals. 1949;**76**:321-360
- [21] Krohn BR. Modern Casting. 1985;**75**:21
- [22] Gruzleski JE, Closset BM. The Treatment of Liquid Aluminum-Silicon Alloys. Des Plaines, Illinois, USA: AFS; 1990
- [23] Tenekedjiev N, Mulazimoglu H, Closset B, Gruzleski J. Microstructures and Thermal Analysis of Strontium-Treated Aluminum-Silicon Alloys. Des Plaines, Illinois, USA: AFS; 1995. pp. 40-41
- [24] Ananthanarayanan L, Gruzleski JE. AFS Transactions. 1992;**141**:383-391
- [25] Sparkman DA. AFS Transactions. 2011;**1199**:1-8
- [26] Upadhyaya KG, Stefanescu DM, Lieu K, Yeager DP. AFS Transactions. 1989;**47**:61-66
- [27] Apelian B, Sigworth GR, Wahler KR. AFS Transactions. 1984;**161**: 297-307
- [28] Djurdjevic MB, Kasprzak W, Kierkus CA, Kierkus WT, Sokolowski JH. Quantification of Cu enriched phases in synthetic 3xx aluminum alloys using the thermal analysis technique. AFS Transactions. 2001;**24**:1-8
- [29] Fras E, Kapturkiewicz W, Burbielko A, Lopez HF. AFS. 1993;**101**: 505-511
- [30] Kierkus WT, Sokolowski JH. AFS Transactions. 1999;**66**:161-167
- [31] Cáceres CH, Djurdjevic MB, Stockwell TJ, Sokolowski JH. Scripta Materialia. 1999;**40**(5):631-637
- [32] Cho JI, Jeong CY, Kim YC, Choi SW, Kang CS. The effect of Cu on feeding characteristics of aluminum casting alloys. In: Proceedings of the 12th International Conference on Aluminium Alloys. September 5–9, Yokohama, Japan, Japan Institute of Light Metals. 2010. pp. 745-750
- [33] Chai G. Dendrite coherency during equiaxed solidification in aluminum alloys. In: Chemical Communications., No. 1. Stockholm University: Stockholm, Sweden. p. 1994
- [34] Chai G, Bäckerud L, Rolland T, Arnberg L. Metallurgical and Materials Transactions A: Physical Metallurgy and Materials Science. 1995;**26A**:965-970
- [35] Claxton R. Journal of Metals. 1975; **27**(2):14-16
- [36] Arnberg L, Chai G, Bäckerud L. Materials Science and Engineering A. 1993;**173**:101-103
- [37] Veldman N, Dahle A, John D. St: Determination of dendrite coherency point. In: Proceedings of the Die Casting & Tooling Technology Conference; 22–25 June, Melbourne, Australia. 1997
- [38] Tamminen J. Thermal analysis for investigation of solidification mechanisms in metals and alloys. In: Chemical Communications. Vol. 2. Stockholm, Sweden: Stockholm University; 1988
- [39] Jiang H, Kierkus WT, Sokolowski JH. Dendrite coherency point determination using thermal analysis and rheological measurements. In: Proceedings of TPPM '99, The International Conference on Thermophysical Properties of Materials, 17–19 November 1999, Singapore. 1999
- [40] Zamarripa RC, Ramos-Salas JA, Talamantes-Silva J, Valtierra S, Colas R. Metallurgical and Materials Transactions A: Physical Metallurgy and Materials Science. 2007;**38A**:1875-1879
- [41] Djurdjevic MB, Byczynski G. The impact of chemistry on the dendrite

coherency point of the 3XX series of Al alloys. In: Proceedings of ICAA\_11; vol. 1. September, Aachen, Germany. 2008. pp. 1-12

[42] Arnberg L, Dahle A, Paradies C, Syvertsen F. AFS Transactions. 1995;**115**: 753-759

[43] Flemings MC. Solidification Processing. New York: McGraw-Hill Inc.; 1974. pp. 60-166

[44] Ohta S, Asai K. Transactions of the Japan Welding Society. 1993;**24**(2): 131-139

[45] Saunders N. Materials Science Forum. 1996;**217**(2):667-672

[46] Chen JH, Tsai HL. AFS Transactions. 1990;**98**:539-546

[47] Kantekar CS, Stefanescu DM. AFS Transactions. 1988;**60**:591-598

[48] Huang H, Suri VK, Hill JL, Berry JT. AFS Transactions. 1991;**54**:685-689

[49] Rapaz M. International Materials Reviews. 1989;**34**(3):93-123

[50] Stefanescu DM, Upadhyay G, Bandyopaadhyay D. Metallurgical and Materials Transactions A: Physical Metallurgy and Materials Science. 1990; **2**:997-1005

[51] Jeng S, Chai S. Materials Science Forum. 1996;**217**:283-288

[52] Emadi D, Whiting L, Djurdjevic MB, Kierkus W, Sokolowski J. Metallurgical and Materials Engineering. 2004;**10**:91-106